Cellular Microbiology (2008) **10**(1), 165–176

doi:10.1111/j.1462-5822.2007.01027.x
First published online 14 August 2007

West Nile virus capsid protein induces p53-mediated apoptosis via the sequestration of HDM2 to the nucleolus

Mi-Ran Yang,[1] Sung Ryul Lee,[2] Wonkyung Oh,[1] Eun-Woo Lee,[1] Jung-Yong Yeh,[3] Jin-Ju Nah,[3] Yi-Seok Joo,[3] Jaekyoon Shin,[4] Han-Woong Lee,[5] Suhkneung Pyo[2] and Jaewhan Song[1]*

[1]*Department of Food Science and Biotechnology,*
[2]*College of Pharmacy,* [4]*School of Medicine,*
Sungkyunkwan University, Suwon 440-746, Korea.
[3]*Division of Foreign Animal Disease, National Veterinary Research and Quarantine Service, Anyang 430-824, Korea.*
[5]*Department of Biochemistry, Yonsei University, Seoul 120-749, Korea.*

Summary

The capsid protein of the West Nile virus (WNV) functions as an apoptotic agonist via the induction of mitochondrial dysfunction and the activation of caspases-9 and -3. Here, we have determined that the WNV capsid (WNVCp) is capable of binding to and sequestering HDM2 into the nucleolus. WNVCp was shown to interfere with the formation of the HDM2 and p53 complex, thereby causing the stabilization of p53 and the subsequent induction of its target apoptotic protein, Bax. Whereas WNVCp was capable of inducing the p53-dependent apoptotic process in wild-type mouse embryonic fibroblasts (MEF) or SH-SY5Y cells, it exerted no significant effects on p53-null MEF or on p53-knockdown SH-SY5Y cells. This suggests that WNVCp-mediated apoptosis requires p53. Furthermore, when WNV was transfected into cells, endogenous Hdm2 and WNVCp were able to interact physically. WNVCp expressed in wild-type MEF proved able to induce the translocation of the endogenous Hdm2 into the nucleolus. Consistently, WNV was highly pathogenic in the presence of p53, and was less so in the absence of p53. The results of these studies suggest that the apoptotic mechanism mediated by WNV might occur in accordance in a fashion similar to that of the tumour-suppressing mechanism mediated by ARF.

Received 16 May, 2007; revised 26 June, 2007; accepted 12 July, 2007. *For correspondence. E-mail jso678@skku.edu; Tel. (+82) 31 290 7807; Fax (+82) 31 290 5270.

Introduction

The West Nile virus (WNV) is an arthropod-borne virus in the Flaviridae family, which induces febrile syndrome, meningitis, encephalitis, hepatitis, flaccid paralysis, and even death (Sampson *et al*., 2000). It harbours single-stranded RNA, which encodes for the capsid, envelope, premembrane proteins and seven non-structural proteins that have been implicated in viral replication (Chambers *et al*., 1990). WNV is known to induce Bax-dependent or Bax-independent apoptotic cell death in several cancer and brain cell lines, and in mouse brain and skeletal muscles (Parquet *et al*., 2001; Yang *et al*., 2002; Chu and Ng, 2003; Ramanathan *et al*., 2006). A few factors expressed by the WNV genome, including NS2B–NS3 and WNV capsid (WNVCp), have been shown to participate in WNV-mediated apoptosis (Oh *et al*., 2006a; Ramanathan *et al*., 2006). However, the mechanisms involved directly in these processes have yet to be characterized fully.

As Bax is a transcriptional target of p53, it appears likely that WNV infection may involve a p53-associated mechanism (Miyashita and Reed, 1995). As a tumour suppressor which functions as a transcription factor, p53 is activated in response to oncogenic or DNA-damaging stresses, resulting in cell cycle arrest and apoptosis (Harris and Levine, 2005; Vousden and Prives, 2005). When these surveillance functions of p53 against tumour-inducing factors are lost, cells become predisposed to tumourogenecity (Donehower *et al*., 1992; Christophorou *et al*., 2006). Under normal conditions, p53 accumulation is constantly prevented by HDM2-mediated ubiquitination, followed by 26S proteasome-dependent degradation (Haupt *et al*., 1997; Kubbutat *et al*., 1997). HDM2 is also a transcriptional target of p53, which participates in the negative feedback loop of p53 to inhibit abnormal p53 accumulation under normal conditions (Haupt *et al*., 1997). A variety of oncogenic stresses are also known to induce the post-translational modification of p53, resulting in its acetylation, phosphorylation, methylation or sumoylation (Harris and Levine, 2005). These processes appear to prevent direct interactions between p53 and HDM2. Also, the interactions between HDM2 and p53 can be blocked via the inhibitory effects of the ARF tumour suppressor protein ($p14^{ARF}$ and $p19^{ARF}$ for human and

mouse respectively) (Kamijo *et al*., 1998; Sherr and Weber, 2000). ARF, which is activated by oncoproteins, including E2F-1, Ras or Myc, as well as oncogenic stresses, is located within the nucleolus, and induces the sequestration of HDM2 into the nucleolus via direct interaction (Tao and Levine, 1999; Sherr and Weber, 2000). Thus, stressed conditions prevent HDM2-mediated p53 degradation and result in p53 activation, inducing apoptosis or cell cycle arrest. Mice lacking only *ARF* evidenced spontaneous tumour development with an interruption of the p53-dependent signal transduction pathway, indicating the upstream role of ARF in the process of p53-mediated stress responses (Kamijo *et al*., 1997). Similarly to ARF, ribosomal proteins L11 and L23 also bind to HDM2 and induce its localization into the nucleolus, resulting in the activation of p53 (Lohrum *et al*., 2003; Zhang *et al*., 2003; Jin *et al*., 2004). In addition, PML also sequesters HDM2 into the nucleolus under stressed conditions and increases the stability of p53 (Bernardi *et al*., 2004). Thus, it appears that the nucleolar sequestration of HDM2 is one of the essential strategies utilized for the augmentation of the transcriptional activities of p53.

This study showed that the overexpressed WNVCp, which consistently localized to the nucleolus, was involved in Hdm2 nucleolar localization. The nucleolar colocalization of WNVCp and HDM2 subsequently leads to the stabilization of p53. In accordance with these data, WNVCp was able to mediate apoptosis only in the presence of p53.

Results

West Nile virus capsid stabilizes p53 by preventing its interaction with Hdm2

In previous studies, it was suggested that WNVCp induced apoptosis in cancer cells via caspase-9 activation and mitochondrial dysfunction (Yang *et al*., 2002). As the suggested apoptotic mechanism is closely associated with the Bax-dependent pathway, we attempted to determine whether WNVCp could affect the levels of Bax and its transcriptional activator, p53 (Miyashita and Reed, 1995). The results of this study indicated that ectopic WNVCp expression was capable of inducing the accumulation of p53 and its target proteins, Bax and Hdm2, in U2OS human osteoblastoma cells harbouring normal p53 (Fig. 1A). In SK-N-SH cells, WNVCp also induced p53 overexpression and the cleavage of PARP, an apoptotic marker (Fig. S1A). WNVCp also induced caspase-9 and -3 activation in the same cell lines, as was previously reported (data not shown, and Fig. S1B) (Yang *et al*., 2002). Consistently, WNVCp-mediated caspase-9 and caspase-3 were also activated in AGS cells, which harbour functional p53, but this was not observed in 293T cells, as its p53 was suppressed by the large T antigen (data not shown). p53 accumulation was determined not to be the result of activated transcription, as the mRNA levels of p53 detected via reverse transcription polymerase chain reaction (RT-PCR) were unchanged (data not shown). Although these results show that the WNVCp may post-translationally stabilize p53, this was not found to be the result of any direct interaction occurring between WNVCp and p53, as the proteins did not interact with each other in our system, as was shown by the results of immunoprecipitation (Fig. 1B, lanes 1 and 2). Interestingly, the ectopic expression of WNVCp was capable of reducing the HDM2-mediated ubiquitination of p53 (Fig. 1C, lanes 4 and 5). These results prompted us to attempt to determine whether WNVCp could regulate the E3 ligase activities of HDM2 via direct interaction. Immunoprecipitation and GST-pulldown assays indicated that WNVCp and HDM2 could bind directly (Fig. 1D and F, lane 5). Mdm2, which is a mouse Hdm2, was also capable of interacting with WNVCp (Fig. 1E). Furthermore, exogenous HDM2 was stabilized by WNVCp in the H1299 cell line, which lacks HDM2's transcriptional activator, p53 (Fig. 2A). The reduction of HDM2 self-ubiquitination in the presence of WNVCp shows that WNVCp could inhibit E3 ligase activities via direct interaction (Fig. 2B, lane 4).

We then co-transfected plasmids expressing HDM2 and WNVCp into U2OS cells in order to demonstrate whether the stabilization of endogenous p53 was accomplished via the WNVCp-induced inhibition of HDM2-mediated p53 degradation. HDM2 overexpressed alone in the cells effected a reduction in p53 levels, whereas the addition of WNVCp prevented the HDM2-mediated depletion of p53 (Fig. 2C, lane 3). Using immunoprecipitation assays, WNVCp was determined to interfere with the physical interaction between HDM2 and p53 (Fig. 2D, lanes 3–5). Taken together, our results indicated that WNVCp was capable of inhibiting and stabilizing HDM2 via direct interaction with it. As a result, p53 was stabilized and activated, which resulted in the expression of Bax and the activation of caspase-9 and caspase-3.

West Nile virus capsid could sequester HDM2 into the nucleolus in an ARF-independent manner

As exogenous WNVCp was localized to the nucleolus, we then attempted to determine whether WNVCp was capable of affecting the cellular localization of HDM2 (Yang *et al*., 2002; Oh *et al*., 2006a). The localization of WNVCp into the nucleolus was verified by observing that WNVCp colocalized with a nucleolar protein, nucleolin, in U2OS (Fig. 3A, panels 1–4). WNVCp was also capable of localizing to the nucleoli in SK-N-SH, H1299, 293T and mouse embryonic fibroblasts (MEF) (data not shown). However, HDM2 expressed alone remained in the nucleo-

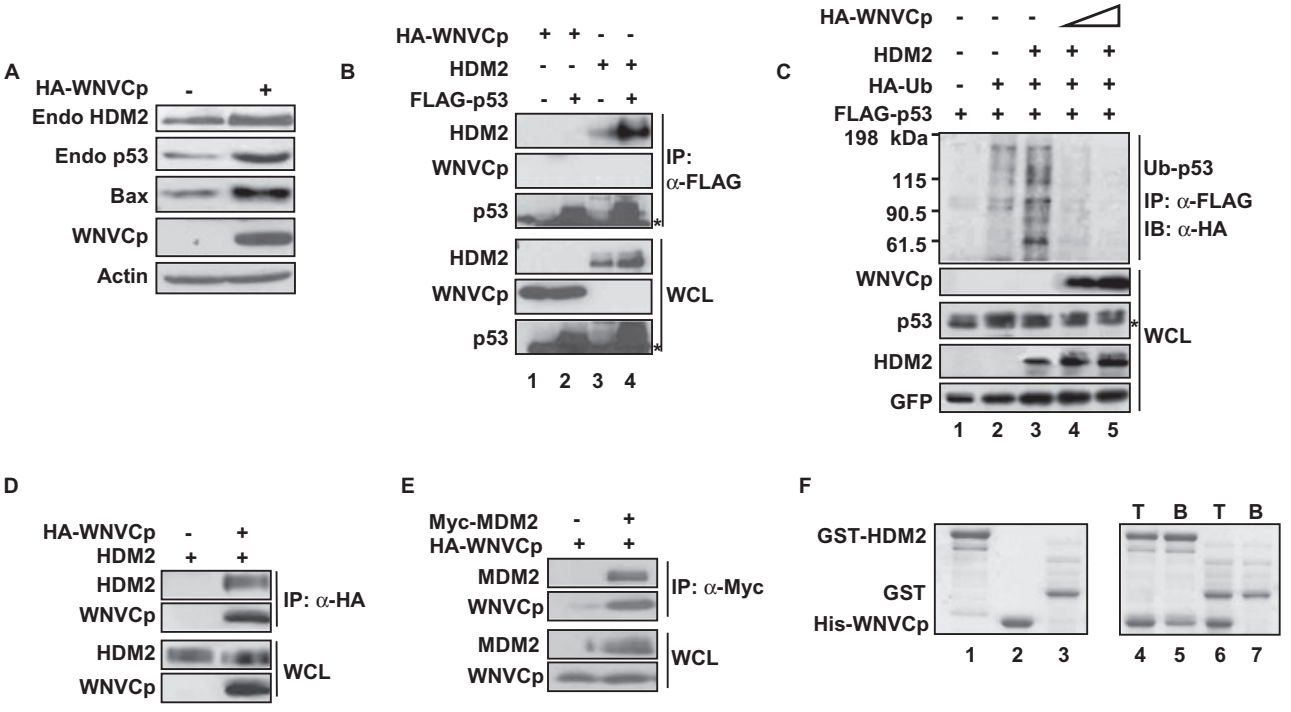

Fig. 1. WNVCp stabilizes p53 by inhibiting its ubiquitination by HDM2.
A. The HA-WNVCp-expressing plasmids were transfected into U2OS cells. The whole-cell lysates (WCL) were then resolved via SDS-PAGE and processed for Western blotting with monoclonal anti-HA, anti-HDM2, anti-p53 and anti-actin mouse antibodies and polyclonal anti-Bax rabbit antibodies.
B. Empty vector or plasmids expressing FLAG-p53, HA-WNVCp or HDM2 were transfected into 293T cells. The cell lysates were then immunoprecipitated using monoclonal anti-FLAG mouse antibodies. The WCL and immunoprecipitated samples (IP) were detected using monoclonal anti-HDM2 and anti-HA mouse and polyclonal anti-p53 rabbit antibodies. The endogenous p53 is indicated by an asterisk.
C. 293T cells were transfected with a combination of plasmids expressing HA-WNVCp, HDM2, HA-Ub, FLAG-p53 or GFP, with or without empty vector. The cell lysates were then immunoprecipitated using anti-FLAG mouse antibodies. WCL was detected with anti-HA, anti-HDM2, anti-p53 and anti-FLAG mouse, and anti-GFP rabbit antibodies. Ubiquitinated p53 was immunoprecipitated and then detected with anti-HA rabbit antibodies. The endogenous p53 is indicated by an asterisk.
D. Plasmids expressing HA-WNVCp and HDM2 were co-transfected into 293T cells. The cell lysates were immunoprecipitated using anti-HA mouse antibodies. WCL and IP were detected by anti-HA and anti-HDM2 mouse antibodies.
E. Plasmids expressing HA-WNVCp and Myc-MDM2 were co-transfected into 293T cells. The cell lysates were immunoprecipitated using anti-Myc mouse antibodies. And WCL and IP were detected by anti-HA and anti-Myc mouse antibodies.
F. Purified GST-HDM2, GST and His-WNVCp were resolved via 12% SDS-PAGE, followed by Coomassie blue staining (lanes 1–3). His-WNVCp was incubated either with GST-HDM2 or GST [T (total), lanes 4 and 6]. Proteins bound to glutathione-sepharose beads [B (bound), lanes 5 and 7] were pelleted, eluted and resolved as described above.

plasm, as has been reported in previous studies (Fig. 3A, panels 5 and 6) (Tao and Levine, 1999). Upon the coexpression of HDM2 and WNVCp, both proteins were localized in the nucleoli in U2OS, as well as the other cancer cell lines mentioned above (Fig. 3B, panels 1–12, and data not shown). Similarly, the nucleolar colocalization of exogenous WNVCp and endogenous HDM2 was observed in U2OS (Fig. 3B, panels 13–16). Interestingly, when WNVCp was exogenously expressed, approximately 50% of the cells evidence a localization of WNVCp in both the nucleolus and the cytoplasm, thereby indicating that WNVCp is not entirely restricted to the nucleolus as the result of artificial overexpression (Fig. 3B, panels 5–8). Overall, WNVCp was capable of sequestering HDM2 into the nucleolus, which would prevent the formation of a complex between HDM2 and p53.

In the presence of oncogenic proteins, including Ras, E2F or c-Myc, all of which induce ARF expression, HDM2 is localized to the nucleolus via direct interaction with ARF (Palmero *et al*., 1998). Thus, we attempted to ascertain whether WNVCp might impose similar oncogenic stress effects, which induce the ARF-dependent re-localization of HDM2 into the nucleolus. In order to determine this, we employed $p19^{ARF}$-null MEF in this study. In these cells, HDM2 alone generally localized to the nucleoplasm was translocated into the nucleoli in the presence of WNVCp (Fig. 4, panels 3–8). As a control experiment, the colocalization of exogenous HDM2 and $p19^{ARF}$ was also detected, as was reported previously (Fig. 4, panels 9–12) (Tao and Levine, 1999). Overall, the results obtained in this study suggest that the WNVCp-mediated translocation of HDM2 into the nucleolus could take place independently of ARF.

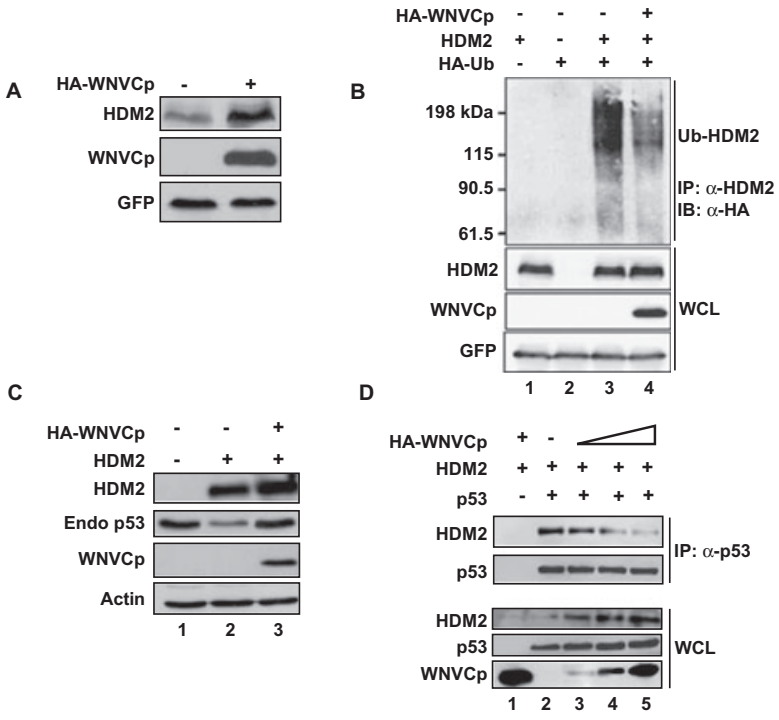

Fig. 2. WNVCp inhibits E3 ligase activity of HDM2 and prevents its interaction with p53.
A. A combination of plasmids expressing HA-WNVCp, GFP and HDM2 were transfected into H1299. The cell lysates were detected as described in Fig. 1A.
B. 293T cells were transfected with combinations of empty vector or plasmids expressing HDM2, HA-WNVCp or HA-Ub. The cell lysates were immunoprecipitated with anti-HDM2 mouse antibodies and detected using anti-HA rabbit antibodies. WCL were detected as described above.
C. U2OS cells were transfected using plasmids expressing HDM2, HA-WNVCp or both. Cell lysates were immunoblotted with anti-HA, anti-HDM2 and anti-actin mouse, and anti-p53 rabbit antibodies.
D. H1299 cells were transfected using p53- and HDM2-expressing plasmids with increasing amounts of HA-WNVCp (1, 2, 4 μg) (lanes 3–5) or empty vector (4 μg) (lane 2). The cell lysates were immunoprecipitated using anti-p53 rabbit antibodies. WCL and IP were detected by anti-HA, anti-p53 and anti-HDM2 mouse antibodies.

The C-terminus of WNVCp is required for WNVCp's interaction with Hdm2

The C-terminus of WNVCp has been shown to mediate cytotoxic effects on cells (Yang *et al.*, 2002; Oh *et al.*, 2006a). Thus, the WNVCp mutant lacking the C-terminal region of WNVCp, Δ106-123, was assessed with regard to its interaction with HDM2 (Fig. 5). The mutant Δ106-123 proved unable to induce the translocalization of HDM2 into the nucleolus (Fig. 5A, panels 11–14). This mutant proved consistently unable to bind to HDM2, and also proved incapable of inducing p53 and Bax, which suggests that the C-terminus is responsible for WNVCp's cytotoxic effects (Fig. 5B, lane 6 and 5C, lane 4). These results indicated that the C-terminus of WNVCp is responsible for its interaction with HDM2, and is required for its cytotoxic effects on cancer cell lines.

West Nile virus capsid could mediate the apoptotic process in a p53-dependent manner

If WNVCp proved able to mediate p53-dependent apoptosis via the inhibition of HDM2, WNVCp should be defective in displaying apoptotic effects in the absence of p53. In order to determine this, WNVCp was transfected into the wild-type or p53-null MEF, then evaluated with regard to its apoptotic influences. The results indicated that WNVCp was capable of inducing p53 and its target protein, Bax, in wild-type MEF but not in p53-null cells. Furthermore, caspase-9 and caspase-3 were activated only in wild-type MEF. The cleaved PARP, the target of caspase-3, was also observed only in the wild-type (Fig. 6A, lane 2). Caspase-9 and caspase-3 activation were confirmed further by monitoring the cleavage of its colorimetric substrate of caspase-9 and -3 (data not shown). Finally, we conducted FITC-Annexin V and propidium iodide (PI) double staining in order to detect apoptotic cell death via FACS analysis. The data indicated that the transfection of WNVCp induced Annexin V staining in 40% of the wild-type MEF, whereas it exerted no effects on p53-null MEF. When Bax was overexpressed as a control in both cell lines, it induced apoptosis with or without p53, as had been expected (Fig. 6B). This indicates that apoptosis via WNVCp occurred only in the wild-type MEF. As neural cells are quite susceptible to the pathogenic effects of WNV, we next attempted to determine whether WNVCp was capable of inducing the p53-dependent apoptotic pathway in human neuroblastoma SH-SY5Y cells (SY-control) or SH-SY5Y cells stably transfected with a plasmid that expressed p53 siRNA (SY-p53-siRNA). SY-p53-siRNA cells evidenced reduced levels of p53 (Fig. 6C). When these cells were transfected with EGFP-WNVCp, the SY-control evidenced increased caspase-9 and -3 activities after 24 and 48 h, whereas the SY-p53-siRNA cells were not affected by it (data not shown). The SY-control and SY-p53-siRNA cells were tested further for cell death in the presence or absence of EGFP-WNVCp via measurements of the mitochondria

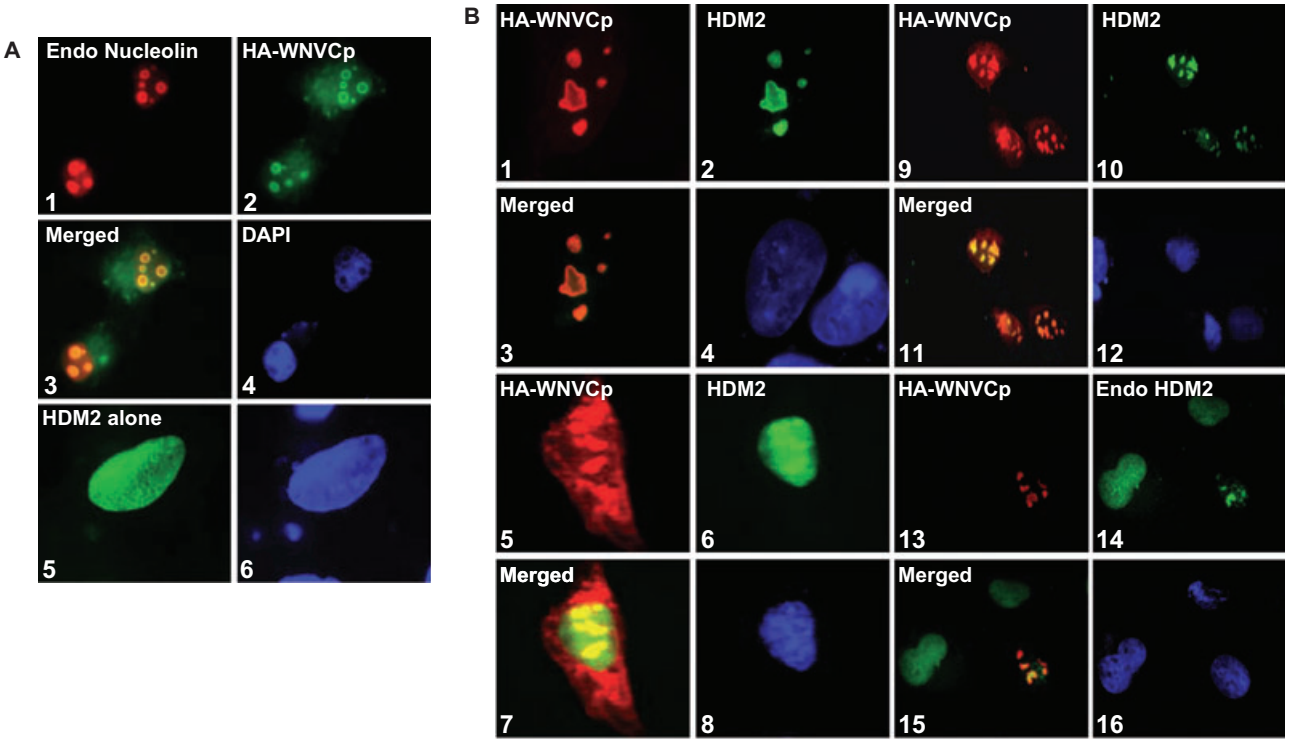

Fig. 3. WNVCp and HDM2 were colocalized in the nucleolus.
A. The U2OS cells were transfected with plasmids expressing HA-WNVCp (panels 1–4) or HDM2 (panels 5 and 6). Twenty-four hours after transfection, cells were fixed and stained with monoclonal anti-HA or anti-HDM2, followed by Alexa Fluor 488-conjugated anti-mouse antibodies (panels 2, 3 and 5), and polyclonal anti-nucleolin, followed by Alexa Fluor 594-conjugated anti-rabbit antibodies (panels 1 and 3).
B. The U2OS cells, which were transfected with plasmids expressing HA-WNVCp and HDM2 (panels 1–12) or HA-WNVCp alone (panels 13–16), were detected using polyclonal anti-HA and the Alexa Fluor 594-conjugated anti-rabbit antibodies and monoclonal anti-HDM2 and the Alexa Fluor 488-conjugated anti-mouse antibodies (panels 1–16). The cells were counterstained with DAPI in order to visualize the nuclei. The images were captured by immunofluorescence microscopy at ×400 (panels 9–16) or ×1000 (panels 1–8) magnification.

membrane potential (MMP) or the PI uptake in live cells. Both cells were transfected with plasmids expressing either EGFP-WNVCp or EGFP, and the cells expressing EGFP were gated. The shift in MMP was observed only in the SY-control expressing EGFP-WNVCp (Fig. 6D, upper panel, dotted line). A total of 60% of the SY-control cells expressing EFGP-WNVCp consistently evidenced increased PI staining at 48 h, whereas this was only observed in 13% of the SH-SY5Y-p53-siRNA, thereby indicating that the presence of p53 is a prerequisite for WNVCp-mediated cell death (Fig. 6E). When the same experiments were conducted on cell lines containing either functional or non-functional p53, we observed that only the cell lines harbouring functional p53 were stained with PI (data not shown). Collectively, these observations suggested that WNVCp could induce the apoptotic process in a p53-dependent manner.

P53 is required for the effective infection of WNV

The data presented above define the possible functional roles of WNVCp under overexpressed conditions. However, the functional relevancy of WNVCp *in vivo* needs to be addressed in order to understand the role of WNVCp under physiological conditions. In order to ascertain whether WNVCp still carries out the function described above under infectious conditions, we infected mammalian cells with WNV. First, we conducted immunoprecipitation analyses of WNVCp and endogenous Hdm2 using 293T cells infected with WNV. The data indicate that the WNVCp expressed from infected WNV was able to interact with endogenous Hdm2, suggesting a possible *in vivo* regulatory role of WNVCp with regard to the function of Hdm2 (Fig. 7A). We then attempted to determine whether WNVCp was capable of inducing the nucleolar localization of endogenous Mdm2 as suggested by *in vitro* analysis using wild-type MEF (Fig. 3B). The results of immunofluorescent analysis indicated that the endogenous Mdm2 alone was localized within the nucleoplasm (Fig. 7B, panels 1 and 2). WNVCp expressed from the WNV infection was principally localized in the cytoplasm and nucleoli as it colocalized with the nucleolus marker, nucleophosmin (Fig. 7B, panels 3–6). When wild-type MEF cells were infected by WNV,

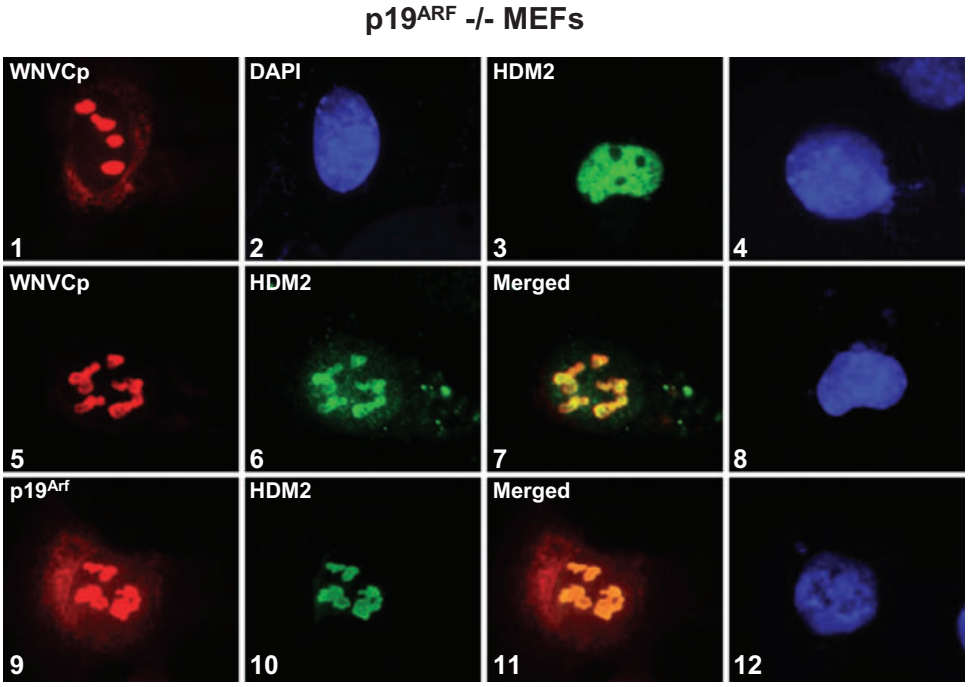

Fig. 4. WNVCp induced the nucleolar localization of HDM2 in an ARF-independent manner. The p19^{ARF}-null MEF, transfected with plasmids expressing HA-WNVCp (panels 1 and 2), HDM2 (panels 3 and 4), HDM2 + WNVCp (panels 5–8) and HDM2+ HA-p19^{ARF} (panels 9–12), were detected as described in Fig. 3.

we observed that WNVCp and endogenous Mdm2 were colocalized in the nucleolus. These results indicate that WNVCp and endogenous Mdm2 are able to interact *in vivo*, which might facilitate the induction of p53 due to the inhibition of endogenous Mdm2. To further test this, wild-type or p53-null MEF cells were infected using WNV, and its effects on both cell lines were monitored. The infection of WNV on the wild-type MEF led to the induction of p53 and its target proteins, Bax and p21, but exerted no effects on p53-null cells (Fig. 7C). Consistently, the propagation of WNV in p53-null cells was significantly less efficient than was observed in the wild-type, as shown by the lower amount of WNVCp detected, as is shown in Fig. 7C. The importance of p53 in the induction of cell death via WNV infection was obvious when the cell cycle of each cell line infected with WNV was characterized using FACS analysis (Fig. 7D). While the infection of cells using low doses of WNV exerted no apparent effects on p53-null cells, it induced the cell cycle arrest of wild-type MEF cells at the G_1 phase. When high doses of WNV were applied to each of the cell lines, cell death was observed principally in the wild-type MEF, whereas the p53-null cells were arrested principally at the G_1 phase. These data are consistent with the induction of p53 and its targets, p21 and Bax, under WNV infection conditions. Overall, the above-described *in vivo* observations suggested that biologically relevant WNVCp could indeed interact with endogenous Mdm2, and that this interaction might result in the induction of p53, which resulted in cell cycle arrest or death.

Discussion

The molecular mechanisms of cell death induced by WNV infection remain largely unknown. The infectious dose of WNV to cells has been shown to be responsible for the characterization of cellular necrotic or apoptotic processes (Chu and Ng, 2003). While a high level of viraemia in WNV infection might induce necrosis, treatments at low doses induced apoptosis via the annihilation of mitochondrial function, subsequent cytochrome *c* release and caspase-9 activation. Furthermore, it was suggested that WNV infection of cells might result in an upregulation of the levels of Bax, which is a target of the transcriptional factor, p53 (Parquet *et al.*, 2001). Several WNV proteins have been implicated in the apoptotic processes induced upon infection. For example, members of the WNV's non-structural proteins, the NS2B–NS3 complex, were shown to induce the activation of caspase-8 in host cells, which results in their apoptosis. NS3 protease, and its cofactor NS2B, which are expressed in all of the Flaviviruses, including the Dengue and Langat viruses, evidence functional homology across species (Ramanathan *et al.*, 2006). The capsid protein of WNV is another factor that has been shown to induce apoptosis via the activation of

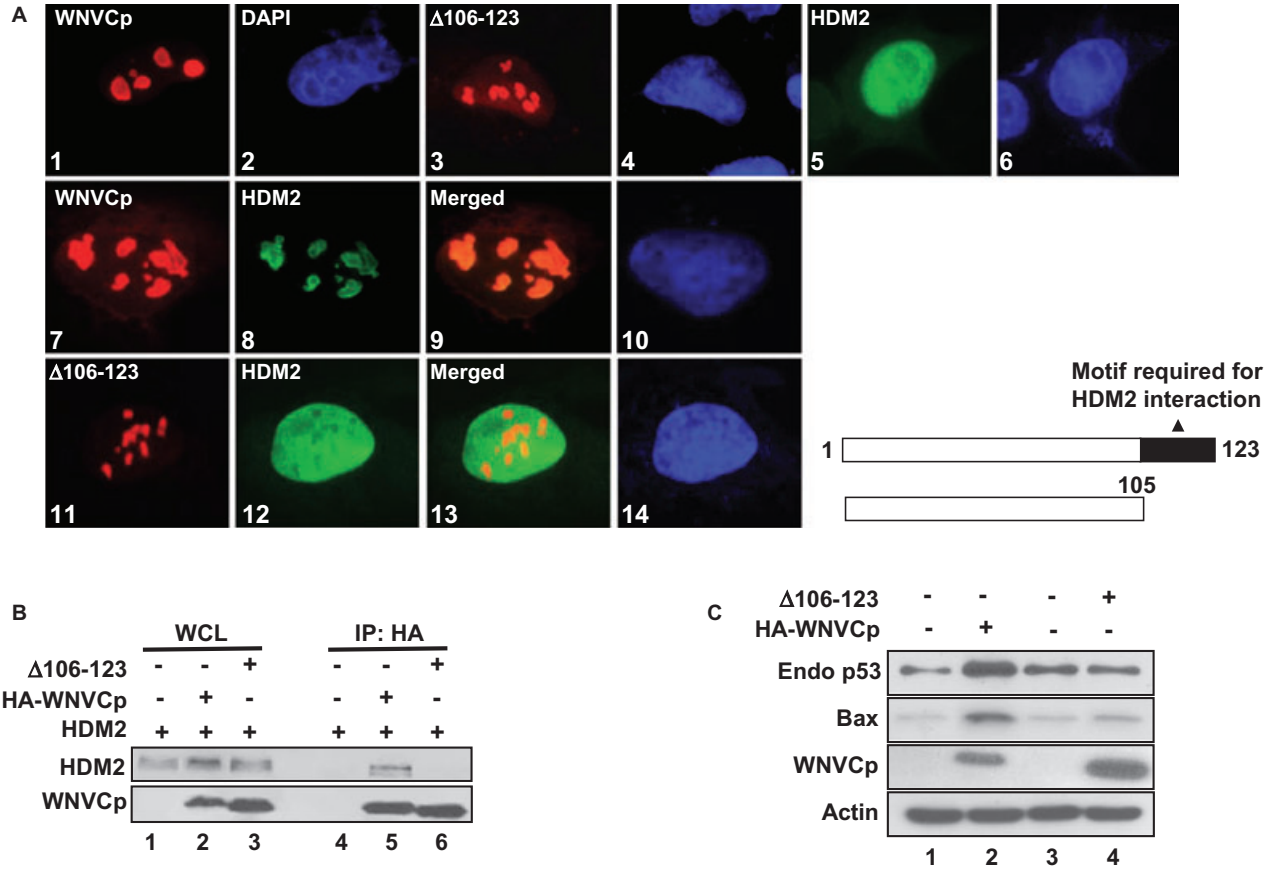

Fig. 5. The C-terminus of WNVCp is required for its interaction with HDM2.
A. The U2OS were transfected with plasmids expressing HA-WNVCp (panels 1 and 2), HA-Δ106-123 (panels 3 and 4), HDM2 (panels 5 and 6), HA-WNVCp + HDM2 (panels 7–10), or HA-Δ106-123 + HDM2 (panels 11–14). The transfected cells were detected as described in Fig. 2. The schematic of the full-length and the C-terminal deletion mutant (Δ106-123) of WNVCp is shown.
B. The empty vector or plasmids expressing the combination of HA-WNVCp, HA-Δ106-123 or HDM2 were cotransfected into 293T cells. The cell lysates were immunoprecipitated using anti-HA mouse antibodies. WCL and IP were detected using anti-HA rabbit and anti-HDM2 mouse antibodies.
C. U2OS cells were transfected with HA-WNVCp or HA-Δ106-123. Cell lysates were detected as described in Fig. 1A.

caspase-9 and caspase-3 and the disruption of mitochondrial function (Yang *et al*., 2002; Oh *et al*., 2006a). Thus, it has been established that WNV can induce the extrinsic or intrinsic apoptotic pathways mediated by the activation of caspase-8 or caspase-9 respectively.

Although the function of WNVCp as a cellular apoptosis inducer in mammalian cells has been advanced theoretically, the mechanism by which WNVCp might mediate the apoptotic pathway in tissues as well as in cells has yet to be defined. Furthermore, there is as yet no clear explanation as to the manner in which the nucleolar localization of WNVCp might induce apoptotic processes in host cells, as indicated previously (Yang *et al*., 2002; Oh *et al*., 2006a).

p53 is a potent tumour suppressor transcription factor which mediates cell cycle arrest, senescence and apoptosis (Harris and Levine, 2005). The participation of p53 with viral proteins has been identified as important factors in viral propagation. For example, the E6 ligase of the papilloma virus induces the degradation of p53, which results in cervical cancer in the long term (Werness *et al*., 1990). The regulatory mechanism of p53 by the hepatitis C virus NS5A and core proteins appear to play a critical role in finally inducing hepatoma in humans (Otsuka *et al*., 2000; Majumder *et al*., 2001). The simian virus 40 large tumour antigen, which binds to p53, is crucial for the transformation and induction of tumours in animals (Tiemann *et al*., 1995). All of these observations show that the virus was capable of negatively regulating the function of p53 to properly improve viral propagation in animal cells. Thus, it appears that a variety of viruses commonly employ the p53 regulator system for effective survival in nature. The results in this report indicate that WNVCp could also modulate the function of p53 by interaction with and the sequestration of HDM2 into the nucleolus.

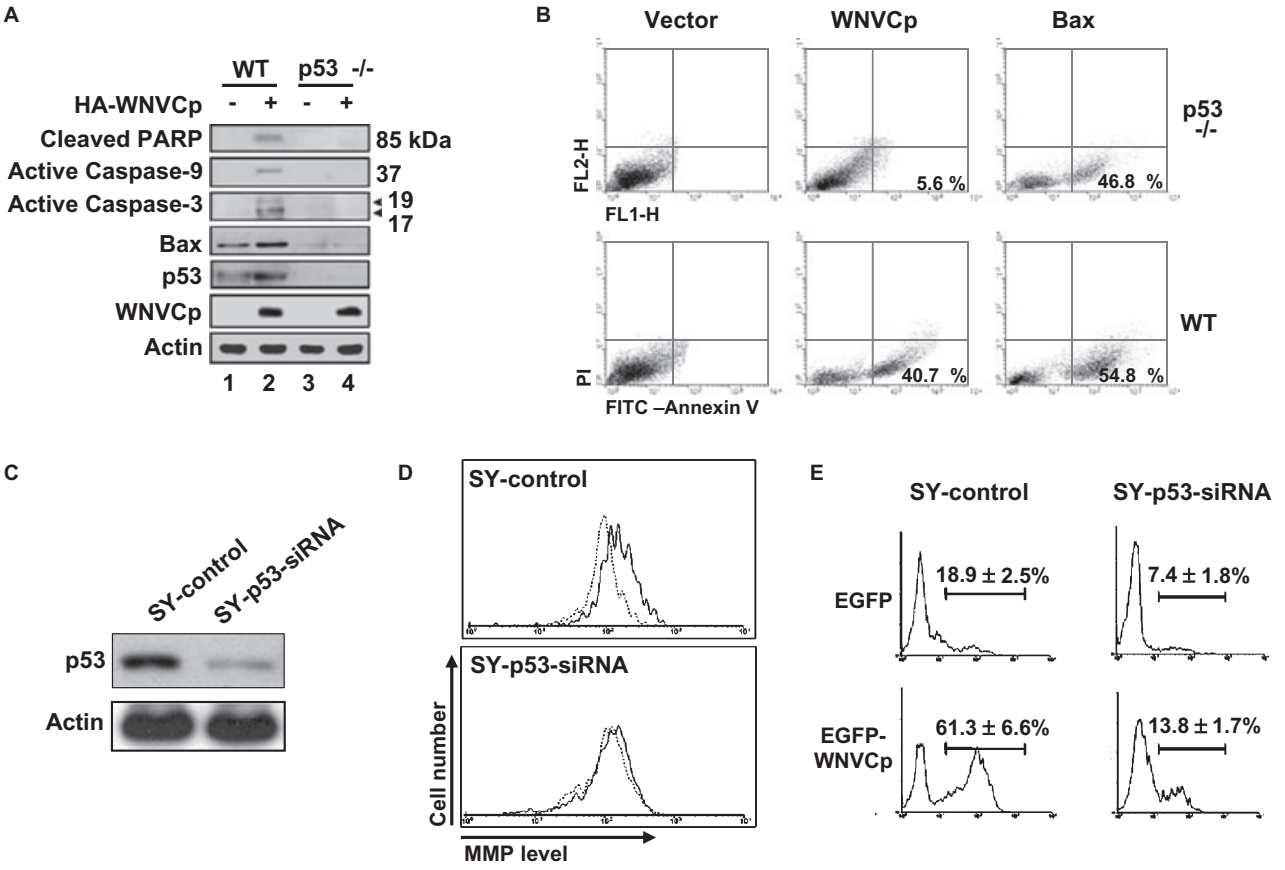

Fig. 6. WNVCp induces p53-dependent apoptosis.
A. Wild-type or p53-null MEF were transfected with plasmids expressing HA-WNVCp or empty vectors. After transfection, cell lysates were detected using anti-HA, anti-actin, anti-p53 and anti-caspase-9 mouse, and anti-Bax, anti-cleaved-caspase-3 and anti-PARP fragment rabbit antibodies.
B. Wild-type or p53-null MEF were transfected with empty vector, or with plasmids expressing HA-WNVCp or Bax. After 24 h, live cells were double-stained with FITC-Annexin V and PI. The stained cells were detected via flow cytometry (WinBRYTE HS, Bio-Rad) and analysed using CellQuest Pro software.
C. The WCL of SH-SY5Y cells (SY-control) or SH-SY5Y cells stably transfected with pSuper-Neo-*p53* (SY-p53-siRNA) were detected using anti-p53 and anti-actin mouse antibodies.
D. SY-control and SY-p53-siRNA cells were transfected with plasmids expressing EGFP (solid line) or EGFP-WNVCp (dotted line). After 48 h, the cells were fixed and stained with Mitotracker red CMXRos. Mitochondrial transmembrane potential (MTP) changes were measured via flow cytometry after gating the EGFP-expressing cells.
E. SY-control and SY-p53-siRNA cells, transfected for 48 h with plasmids expressing EGFP-WNVCp or EGFP, were then suspended and stained with PI. The PI uptake rate was determined via flow cytometry after the EGFP gating and analysed with CellQuest Pro software.

Under normal conditions, p53 is degraded constantly by the presence of its target E3 ligase, Hdm2 (Fig. 8, ①). Upon WNV infection, expressed WNVCp will bind to Hdm2 and chaperone it to the nucleolus (Fig. 8, ③, ④). This prevents the binding of Hdm2 to p53, which results in the stabilization of p53, Bax activation, and subsequent apoptosis (Fig. 8, ⑤, ⑥, ⑦).

West Nile virus capsid was also capable of stabilizing HDM2 via direct interaction (Fig. 2). As the stabilization of HDM2 by ARF was also reported previously, it appears that WNVCp exerts a similar protective effect against HDM2 degradation via the inhibition of the ligase activity of E3 ligase (Kamijo *et al.*, 1998; Honda and Yasuda, 1999). As WNVCp is shown to induce the nucleolar localization of HDM2 in ARF-null MEF, it appears that WNVCp does not require the presence of ARF in order to negatively regulate HDM2 (Fig. 4). We determined that all of these functional characteristics of WNVCp were quite similar to those of ARF. However, when the sequence homology between WNVCp and ARF was examined, we determined there to be no structural similarity between the two proteins, thereby suggesting that the two distinguished proteins share a similar pathway for the inhibition of HDM2 function.

The C-terminal deletion mutant of WNVCp neither interacted with nor sequestered HDM2 into the nucleolus. These results are also consistent with the previous observation, which resulted in the conclusion that the

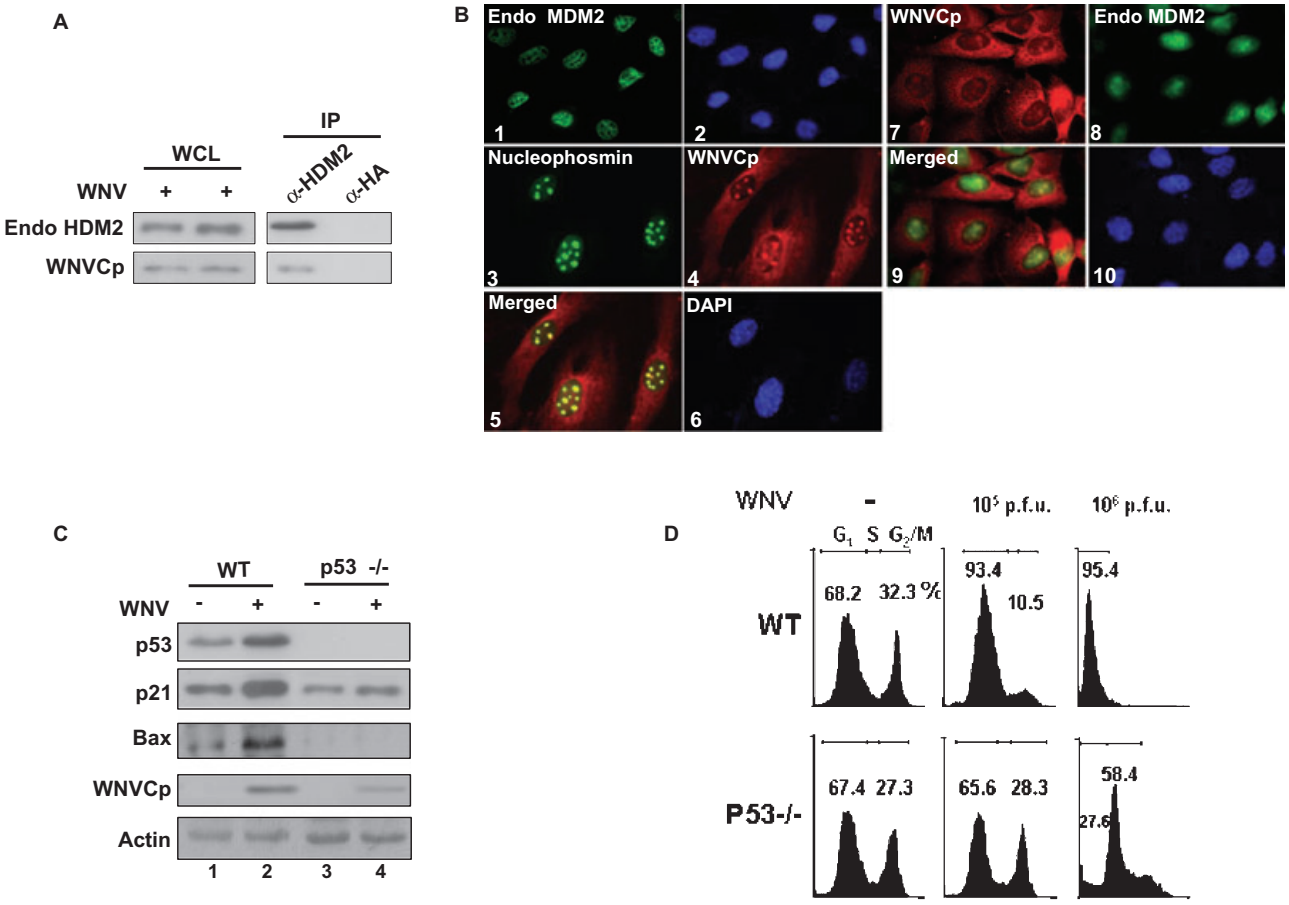

Fig. 7. Hdm2 is translocated into the nucleolus upon WNV infection in wild-type MEF cells.
A. WNV (10^6 pfu) was infected into 293T cells. The whole-cell lysates (WCL) were then resolved via SDS-PAGE and processed for Western blotting with monoclonal anti-HA, anti-Hdm2, anti-p53 and anti-actin mouse antibodies, and polyclonal anti-Bax rabbit antibodies. Plasmids expressing HA-WNVCp and HDM2 were co-transfected into 293T cells. The cell lysates were immunoprecipitated using anti-HA mouse antibodies. WCL and IP were detected by anti-HA and anti-HDM2 mouse antibodies.
B. The MEF cells were infected with WNV (10^5 pfu). Forty-eight hours after infection, the cells were fixed and stained with monoclonal anti-nucleophosmin and anti-HDM2 or polyclonal anti-WNVCp, followed by Alexa Fluor 488-conjugated anti-mouse antibodies (panels 1, 3 and 8), or Alexa Fluor 594-conjugated anti-rabbit antibodies (panels 4 and 7). The cells were counterstained with DAPI in order to visualize the nuclei.
C. Wild-type or p53-null MEF were infected WNV (10^5 pfu). After 72 h, the cell lysates were detected using anti-p53, anti-p21 and anti-actin mouse, and anti-Bax and anti-WNVCp rabbit antibodies.
D. Wild-type or p53-null MEF were infected with WNV 10^5 or 10^6 pfu. After 72 h, the cells were fixed with ethanol followed by PI staining. The stained cells were detected via flow cytometry (WinBRYTE HS, Bio-Rad) and analysed using CellQuest Pro software.

C-terminus of WNVCp was responsible for its cytotoxic effects (Oh *et al*., 2006a; Yang *et al*., 2002). Furthermore, this observation suggests that the translocalization of Hdm2 into the nucleolus by WNVCp is required for the negative regulation of p53. As the small peptide group of the last 18 amino acids of WNVCp appears to be responsible for its interaction with HDM2, we expect that it may prove possible to develop a novel peptide, which can then be employed as an inhibitor of the interaction between HDM2 and p53.

The observation of physiological interaction between endogenous Mdm2 and WNVCp directly expressed as the result of WNV infection verifies that the observations made using the overexpressed system are indeed physiologically relevant (Fig. 7). Furthermore, WNV was effective in inducing cell death only with cell lines harbouring intact p53. When p53 was not present, WNV was incapable of inducing efficient cell death or cell cycle arrest, both of which are important for viral propagation. These observations indicate that WNV requires a pathway that will somehow affect the induction of p53. We suggest here that one of the pathways that WNV exploits for the induction of p53 is the arrest of Hdm2 in the nucleolus by WNVCp. Thus, p53 is no longer inhibited by Hdm2 and becomes able to induce cell cycle arrest or death via the induction of its target genes (Fig. 8).

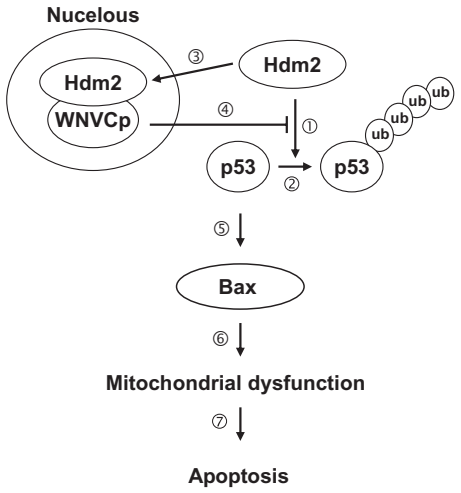

Fig. 8. Schematic diagram of WNVCp interaction with Hdm2. WNV infection induces the direct binding of WNVCp and Hdm2, which results in p53 stabilization. The stabilized p53 subsequently induced the apoptotic signalling pathway, resulting in cellular apoptosis.

It has also been previously determined that viral proteins are localized to the nucleolus for the purpose of viral propagation. For example, the coronavirus or human hepatitis B virus harbour the N protein or Capsid protein respectively. These proteins are located within the nucleolus, which eventually can disrupt cytokinesis of host cells and facilitate the propagation of viral progeny (Hiscox *et al*., 2001; Ning and Shih, 2004). Thus, it seems likely that WNV might employ a strategy similar to the one described above via the localization of its capsid protein into the nucleolus, and may also control the cytokinesis of host cells. Still, our findings indicate an intriguing pathway by which viral proteins could evolutionally mimic and adapt to the biochemical processes of host cells, in order to regulate their cellular fate.

In summary, this is the first report, to our knowledge, to address the manner by which a protein expressed by WNV might induce apoptosis in host cells. This novel pathway may shed new light into the mechanisms underlying the participation of WNV proteins in the transduction signalling pathway of host cells, and may also provide a novel therapeutic target for the pathogenic processes associated with WNV.

Experimental procedures

Plasmids

pGEX-4T1-*HDM2* was kindly provided by E. J. Choi (University of Korea). pcDNA3-HA-*WNVCp* and pET28a-His-*WNVCp* were prepared via the subcloning of an EcoRI/XhoI fragment from pcDNA3-His-*WNVCp* into pcDNA3-HA and pET28a-His (Invitrogen, UK) (Oh *et al*., 2006a). The C-terminal deletion mutant of pcDNA3-HA-*WNVCp* (Δ106-123) was prepared via PCR using pcDNA3-HA-*WNVCp* as a template and the following primers: 5′-ccggaat tcatgtctaaaaaaccaggtggccccgg-3′ (forward) and 5′-acgcgtcgaca gcgcttcttctgcttgct-3′ (reverse). The PCR products were then digested using EcoRI/SalI and cloned into the corresponding sites of the pcDNA3-HA plasmid. Plasmids expressing p53 have been previously reported (Oh *et al*., 2006b). pHM6-HA-*Ub* was used for ubiquitin expression. pEGFP-C2-*WNVCp* was prepared via PCR using pcDNA3-HA-*WNVCp* as a template and the following primer: 5′-ccggaattctctaaaaaaccaggtggccccgg-3′ (forward) and 5′-gactagcggtcgcacccgcgcatcgagctcgcc-3′ (reverse). The PCR products were digested using EcoRI/BamHI and inserted into a pEGFP-C2 plasmid (BD Clontech, San Diego, CA). pSuper-Neo-*p53* was constructed via the insertion of 60 bp of a p53 silencing fragment into the EcoRI/HindIII sites from pSuper-*p53*, then subcloned into the corresponding sites of Super-Neo (Oligoengine, Seattle, WA) (Brummelkamp *et al*., 2002). The resulting plasmid constructs were confirmed via sequence analysis. The isolation of total RNA from pools of arteries was conducted using TRIzol (Invitrogen, UK). cDNA was synthesized from 5 μg of total RNA using AccuPower RT Premix (Bioneer, USA). PCR was conducted using AccuPower PCR Premix (Bioneer, USA). The following primers were employed for PCR: 5′–cggaattcccagggagcacta agcga-3′ (forward) and 5′-ccgctcgagtcagtctgagtcaggcccttctgtct-3′ (reverse) for p53, 5′-cggaattcatgcccacccgcgccgtgctg-3′ (forward) and 5′-acgcgtcgacacgcgcccacgctggcgat-3′ (reverse) for HA-WNVCp, and 5′-atcactgccacccagaagac-3′ (forward) and 5′-aga ggcagggatgatgttct -3′ (reverse) for GAPDH.

Cell biology

The p53-null and p19-null MEF were kindly provided by G. Lozano (University of Texas) and G. J. Sherr (St Jude Children's Research Hospital) respectively. H1299 (human lung carcinoma), U2OS (human osteoblast), 293T (human kidney carcinoma), SK-N-SH (human neuroblastoma), MEF (mouse embryo fibroblast), U373MG (human glioblastoma), MG-63 (human osteosarcoma), RAW264.7 (mouse monocyte), p53-null and p19-null MEF cells were maintained in Dulbecco's modified Eagle's Medium supplemented with 10% fetal bovine serum (Hyclone, Logan, UT) and 1% penicillin/streptomycin (Invitrogen, UK). Transient transfections were conducted using Lipofectamine Plus reagent (Invitrogen, UK), Wellfect (Welgene, Valencia, CA) or JetPEI (Polyplus-transfection, CA) in accordance with the manufacturers' instructions. Infection of virus was carried out using 10^5 or 10^6 pfu WNV. Immunoprecipitation and Western Blot analysis were conducted as previously described (Oh *et al*., 2006a). The SY-p53-siRNA cell line construct was prepared via the transfection of SH-SY5Y with pSuper-Neo-*p53*, followed by G418 (500 μg ml^{-1}) used as a selection marker.

Viral infection

Vero cell (ATCC CCL-81) monolayers in 6-well plates were infected with 10-fold dilutions of virus in a-MEM medium (Gibco) for 1 h at 37°C, and then initially overlaid with 1% seaplaque agarose (TaKaRa). After 72 h of incubation at 37°C, the second overlay with 0.003% neutral red dye (Sigma) was applied for an additional 24 h, after which the total numbers of plaques were counted in the wells, and viral pfu values were calculated.

Protein purification and pulldown assay

GST and GST-HDM2 were prepared as follows. BL21 cells, which were transformed with pGEX-4T1-*HDM2* or pGEX-4T1, were treated with isopropyl 1-thio-D-galactopyranoside (1 mM) at 25°C. The crude extract was then prepared using lysozyme (Sigma). The extract was resolved over a Resource Q (35 ml; Amersham Biosciences), glutathione agarose (20 ml; Invitrogen) and DEAE column (50 ml; Amersham Biosciences). Fractions harbouring GST or GST-HDM2 were concentrated with a Centriprep-30 (Millipore). His-WNVCp was prepared as previously described (Oh *et al*., 2006a). The pulldown procedure was conducted as previously described (Oh *et al*., 2006a).

Immunofluorescence staining

Cells were plated in 6-well plates with coverslips; transfections were conducted using Lipofectamine Plus reagent (Invitrogen, UK). For infection of WNV, cells were treated with 10^5 pfu WNV. After 24 h for transfection and 48 h for infection, the cells were fixed with 4% paraformaldehyde solution for 15 min at room temperature, then washed with PBS (Invitrogen, UK), and permeabilized for 15 min with 0.5% Triton X-100 in PBS. The cells were then blocked with 5% bovine serum albumin (Santa Cruz Biotech, Santa Cruz, CA) in PBS for 30 min and incubated overnight with the specific primary antibody at room temperature. The samples were then incubated with Alexa Fluor 488-conjugated anti-mouse or Alexa 594-conjugated anti-rabbit antibodies (each diluted 1:400) for 1 h at room temperature. The cells were then stained for 5 min with DAPI (4, 6-diamidino-2-phenylindole, Sigma). The slides were analysed with immunofluorescent microscopes (5203 Axiophot II, Oberkochen, Germany).

Antibodies and chemicals

Monoclonal anti-HDM2 (SMP-14), anti-p53 (DO-1) and anti-HA (F-7) mouse antibodies, and polyclonal anti-p53 (FL-393), anti-HA (Y-11), anti-Bax (N-20) and anti-GFP (FL) rabbit antibodies were purchased from Santa Cruz Biotechnology (Santa Cruz, CA). The monoclonal anti-FLAG (M2) and anti-actin mouse antibodies, and PI were obtained from Sigma. The Alexa Fluor 488-conjugated anti-mouse and Alexa 594-conjugated anti-rabbit antibodies were obtained from Alexa. Monoclonal anti-caspase-9 (#9504) mouse antibodies and polyclonal anti-cleaved-caspase-3 (#9661) rabbit antibodies were acquired from Cell Signaling Technology. The polyclonal anti-WNVCp antibodies were purchased from ProSci (#3433). The polyclonal Anti-p85 poly (ADP-ribose) polymerase (PARP) fragment mouse antibodies came from Promega.

Cell apoptosis analysis

Cells were harvested and apoptotic cells were identified via FITC-Annexin V and PI double-staining or flow cytometry in accordance with the manufacturer's instructions (BD Pharmingen, San Diego, CA). For PI staining, a variety of cells were also harvested and stained for 15 min using PI (1 μg ml^{-1}). For the MMP assay, harvested cells were fixed with formaldehyde (3.7%, final concentration) and stained with 200 nM mitotracker red CMXRos (Molecular Probes, Oregon) The intensities of the red fluorescence of stained cells after MMP or PI staining were analysed via flow cytometry after gating the transfected cells with EGFP signals. At least 5000 transfected cells were gated and analysed. Caspase-9 and -3 colorimetric assay kits were utilized to investigate caspase-9 and -3 activation (BD Clontech, San Diego, CA). Another method for the colorimetric assays employed Ac-DEVD-pNA and Ac-LEHD-pNA as substrates for caspase-9 and caspase-3 respectively (Calbiochem, San Diego, CA). In brief, the cells were harvested after transfection and lysed with lysis buffer (50 mM Hepes, pH 7.4, 100 mM NaCl, 0.1% CHAPS, 1 mM DTT and 0.1 mM EDTA, 10% glycerol). After 1 min of centrifugation at 10 000 *g* at 4°C, 90 μl of reaction buffer (lysis buffer containing 200 μM Ac-DEVE-pNA, or 200 μM Ac-LEHD-pNA) was added to 10 μl of supernatant, and incubated at 37°C. The protein concentration of the cell lysates was measured using a Bio-RAD protein DC assay kit (Bio-RAD, Hercules, CA). Optical density was measured after 2 h at 405 nm.

Acknowledgements

The authors thank Professor Jin-hyun Ahn and Professor Young-Ki Paik for their valuable discussion and counsel, and a grant from the Samsung Research Fund to Sungkyunkwan University in 2006.

References

Bernardi, R., Scaglioni, P.P., Bergmann, S., Horn, H.F., Vousden, K.H., and Pandolfi, P.P. (2004) PML regulates p53 stability by sequestering Mdm2 to the nucleolus. *Nat Cell Biol* **6:** 665–672.

Brummelkamp, T.R., Bernards, R., and Agami, R. (2002) A system for stable expression of short interfering RNAs in mammalian cells. *Science* **296:** 550–553.

Chambers, T.J., Hahn, C.S., Galler, R., and Rice, C.M. (1990) Flavivirus genome organization, expression, and replication. *Annu Rev Microbiol* **44:** 649–688.

Christophorou, M.A., Ringshausen, I., Finch, A.J., Swigart, L.B., and Evan, G.I. (2006) The pathological response to DNA damage does not contribute to p53-mediated tumour suppression. *Nature* **443:** 214–217.

Chu, J.J., and Ng, M.L. (2003) The mechanism of cell death during West Nile virus infection is dependent on initial infectious dose. *J Gen Virol* **84:** 3305–3314.

Donehower, L.A., Harvey, M., Slagle, B.L., McArthur, M.J., Montgomery, C.A., Jr, Butel, J.S., and Bradley, A. (1992) Mice deficient for p53 are developmentally normal but susceptible to spontaneous tumours. *Nature* **356:** 215–221.

Harris, S.L., and Levine, A.J. (2005) The p53 pathway: positive and negative feedback loops. *Oncogene* **24:** 2899–2908.

Haupt, Y., Maya, R., Kazaz, A., and Oren, M. (1997) Mdm2 promotes the rapid degradation of p53. *Nature* **387:** 296–299.

Hiscox, J.A., Wurm, T., Wilson, L., Britton, P., Cavanagh, D., and Brooks, G. (2001) The coronavirus infectious bronchitis virus nucleoprotein localizes to the nucleolus. *J Virol* **75:** 506–512.

Honda, R., and Yasuda, H. (1999) Association of p19 (ARF)

with Mdm2 inhibits ubiquitin ligase activity of Mdm2 for tumor suppressor p53. *EMBO J* **18:** 22–27.

Jin, A., Itahana, K., O'Keefe, K., and Zhang, Y. (2004) Inhibition of HDM2 and activation of p53 by ribosomal protein L23. *Mol Cell Biol* **24:** 7669–7680.

Kamijo, T., Zindy, F., Roussel, M.F., Quelle, D.E., Downing, J.R., Ashmun, R.A., *et al.* (1997) Tumor suppression at the mouse INK4a locus mediated by the alternative reading frame product p19ARF. *Cell* **91:** 649–659.

Kamijo, T., Weber, J.D., Zambetti, G., Zindy, F., Roussel, M.F., and Sherr, C.J. (1998) Functional and physical interactions of the ARF tumor suppressor with p53 and Mdm2. *Proc Natl Acad Sci USA* **95:** 8292–8297.

Kubbutat, M.H., Jones, S.N., and Vousden, K.H. (1997) Regulation of p53 stability by Mdm2. *Nature* **387:** 299–303.

Lohrum, M.A., Ludwig, R.L., Kubbutat, M.H., Hanlon, M., and Vousden, K.H. (2003) Regulation of HDM2 activity by the ribosomal protein L11. *Cancer Cell* **3:** 577–587.

Majumder, M., Ghosh, A.K., Steele, R., Ray, R., and Ray, R.B. (2001) Hepatitis C virus NS5A physically associates with p53 and regulates p21/waf1 gene expression in a p53-dependent manner. *J Virol* **75:** 1401–1407.

Miyashita, T., and Reed, J.C. (1995) Tumor suppressor p53 is a direct transcriptional activator of the human *bax* gene. *Cell* **80:** 293–299.

Ning, B., and Shih, C. (2004) Nucleolar localization of human hepatitis B virus capsid protein. *J Virol* **78:** 13653–13668.

Oh, W., Yang, M.R., Lee, E.W., Park, K.M., Pyo, S., Yang, J.S., *et al.* (2006a) Jab1 mediates cytoplasmic localization and degradation of west nile virus capsid protein. *J Biol Chem* **281:** 30166–30174.

Oh, W., Lee, E.W., Sung, Y.H., Yang, M.R., Ghim, J., Lee, H.W., and Song, J. (2006b) Jab1 induces the cytoplasmic localization and degradation of p53 in coordination with Hdm2. *J Biol Chem* **281:** 17457–17465.

Otsuka, M., Kato, N., Keng-Hsin Lan, H.Y., Kato, J., Goto, T., Shiratori, Y., and Omata, M. (2000) Hepatitis C virus core protein enhances p53 function through augmentation of DNA binding affinity and transcriptional ability. *J Biol Chem* **275:** 34122–34130.

Palmero, I., Pantoja, C., and Serrano, M. (1998) p19ARF links the tumour suppressor p53 to Ras. *Nature* **395:** 125–126.

Parquet, M.C., Kumatori, A., Hasebe, F., Morita, K., and Igarashi, A. (2001) West Nile virus-induced bax-dependent apoptosis. *FEBS Lett* **500:** 17–24.

Ramanathan, M.P., Chambers, J.A., Pankhong, P., Chattergoon, M., Attatippaholkun, W., Dang, K., *et al.* (2006) Host cell killing by the West Nile Virus NS2B-NS3 proteolytic complex: NS3 alone is sufficient to recruit caspase-8-based apoptotic pathway. *Virology* **345:** 56–72.

Sampson, B.A., Ambrosi, C., Charlot, A., Reiber, K., Veress, J.F., and Armbrustmacher, V. (2000) The pathology of human West Nile Virus infection. *Hum Pathol* **31:** 527–531.

Sherr, C.J., and Weber, J.D. (2000) The ARF/p53 pathway. *Curr Opin Genet Dev* **10:** 94–99.

Tao, W., and Levine, A.J. (1999) P19 (ARF) stabilizes p53 by blocking nucleo-cytoplasmic shuttling of Mdm2. *Proc Natl Acad Sci USA* **96:** 6937–6941.

Tiemann, F., Zerrahn, J., and Deppert, W. (1995) Cooperation of simian virus 40 large and small T antigens in metabolic stabilization of tumor suppressor p53 during cellular transformation. *J Virol* **69:** 6115–6121.

Vousden, K.H., and Prives, C. (2005) P53 and prognosis: new insights and further complexity. *Cell* **120:** 7–10.

Werness, B.A., Levine, A.J., and Howley, P.M. (1990) Association of human papillomavirus types 16 and 18, E6 proteins with p53. *Science* **248:** 76–79.

Yang, J.S., Ramanathan, M.P., Muthumani, K., Choo, A.Y., Jin, S.H., Yu, Q.C., *et al.* (2002) Induction of inflammation by West Nile virus capsid through the caspase-9 apoptotic pathway. *Emerg Infect Dis* **8:** 1379–1384.

Zhang, Y., Wolf, G.W., Bhat, K., Jin, A., Allio, T., Burkhart, W.A., and Xiong, Y. (2003) Ribosomal protein L11 negatively regulates oncoprotein MDM2 and mediates a p53-dependent ribosomal-stress checkpoint pathway. *Mol Cell Biol* **23:** 8902–8912.

Supplementary material

The following supplementary material is available for this article online:

Fig. S1. A. SH-SY5Y cells were transfected with plasmids expressing EGFP or EGFP-WNVCp. After transfection, cell lysates were detected using anti-actin, anti-p53 mouse and anti-PARP fragment rabbit antibodies.

B. The SH-SY5Y cells were transfected with empty vector or plasmids expressing EGFP or EGFP-WNVCp. Caspase-9 and -3 activities in WCL were determined via colorimetric assays that measured the cleavage of DEVD-AMC and LHED-AMC respectively. Activity is expressed as the fold increase over the control (transfected with empty vector). Three independent experiments were conducted, and the SDs are indicated by error bars.

This material is available as part of the online article from: http://www.blackwell-synergy.com/doi/abs/10.1111/j.1462-5822.2007.01027.x

Please note: Blackwell Publishing is not responsible for the content or functionality of any supplementary materials supplied by the authors. Any queries (other than missing material) should be directed to the corresponding author for the article.